The Study and Optimization of New Micropattern Gaseous Detectors for High-Rate Applications

V. Peskov, P. Fonte, M. Danielsson, C. Iacobaeus, J. Ostling, and M. Wallmark

***Abstract*—We performed a new series of systematic studies of gain and rate characteristics of several micropattern gaseous detectors. Extending earlier studies, characteristics were measured at various pressures and gas mixtures at a wide range of primary charges, and also when the whole area of the detectors was irradiated with a high-intensity X-ray beam.**

Several new effects were discovered, common to all tested detectors, which define fundamental limits of operation. The results of these studies allow us to identify several concrete ways of improving the performance of micropattern detectors and to suggest that in some applications, resistive plate chambers may constitute a valid alternative. Being protected from damaging discharges by the resistive electrodes, these detectors feature high gain, high rate capability (10^5 Hz/mm^2), good position resolution (better than 30 μm), and excellent timing (50 ps σ).

***Index Terms*—Capillary, micropattern gaseous detectors, resistive plate chambers.**

I. INTRODUCTION

IN THE LAST decade, there was a chain of inventions of new micropattern gaseous detectors: MSGC, CAT, GEM, MICROMEGAS, and many others (see [1], [2], and [24]). Due to their promising properties, especially a potential capability for an excellent position resolution, they were almost immediately adopted as tracker devices for some large-scale experiments at CERN and elsewhere. However, as was later discovered, all micropattern gaseous detectors suffer from two main problems: the maximum achievable gain drops with the counting rate and in the presence of heavily ionizing particles [3]–[5]. The recent experience of the CMS and HERA-B tracker detectors shows that one should take these problems very seriously [6], [7].

Extending our earlier studies, in this study we performed further systematic measurements of the gain characteristics of micropattern gaseous detectors as a function of the amount of primary charge, counting rate, number of amplification steps, and gas pressure in order to obtain some strategic guide for their improvement.

Manuscript received November 5, 2000; revised February 8, 2001.

V. Peskov and M. Danielsson are with the Physics Department, Royal Institute of Technology, Stockholm 10405, Sweden (e-mail: vladimir.peskov@cern.ch).

P. Fonte is with Instituto Superior de Engenharia de Coimbra (ISEC), Portugal, and the Laboratório de Instrumentação e Física Experimental de Partículas (LIP), Coimbra, Portugal.

C. Iakobaeus is with the Karolinska Institute, Stockholm, Sweden.

J. Ostling and M. Wallmark are with the Royal Institute of Technology, Stockholm, Sweden and the Karolinska Institute, Stockholm, Sweden.

Publisher Item Identifier S 0018-9499(01)06973-8.

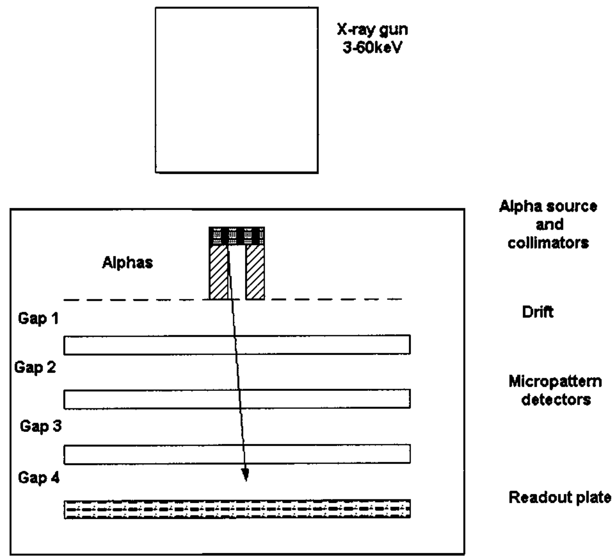

Fig. 1. Schematic drawing of the experimental setup.

II. EXPERIMENTAL SETUP

The experimental setup (Fig. 1) was similar to the one described in [3], [4], [8], and [9] except for two modifications: elevated pressures, up to 10 atm, were possible and a much more powerful X-ray gun was available, allowing exposure of the detectors to counting rates larger than 10^5 Hz/mm^2 over the whole active area of 10 cm $\times$ 10 cm^2.

The following micropattern detectors were tested: MSGC, MICROMEGAS, GEM, CAT, MICRODOT, and glass capillary plate [10], as well as a set of parallel-plate avalanche chambers (PPACs) and resistive plate chambers (RPCs) with gaps varying from 0.1 to 3 mm. The tests were done with single- or few-step configurations.

The MSGCs used were manufactured on Desag glass with electrodes made of chromium and placed at 0.2-, 1-, 3-, or 5-mm pitches. All anode strips were 10 μm wide.

Several MICROMEGAS designs were tested: a commercial design had an anode plate made of printed circuit board with copper strips at a pitch of 300 μm; the others were manufactured by the authors (see [11] for more details).

The GEMs were obtained from CERN and had a rather standard geometry: holes of 100-μm diameter at 140-μm pitch. The CAT was constructed from a GEM whose the anode was kept in contact with a metallic plate.

MICRODOT detectors were custom-made on G10 board with anode and cathode diameters of 30 and 300 μm, respectively.

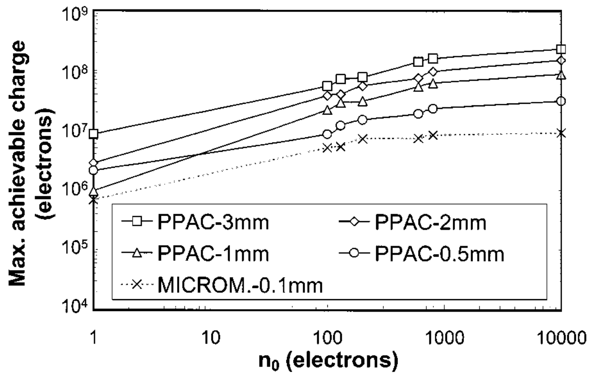

Fig. 2. Dependence of the maximum achievable charge on n_0 for PPAC and MICROMEGAS. The measurements with PPAC were done in Ar+10% ethane and with MICROMEGAS in Ar+4%DME at 1 atm.

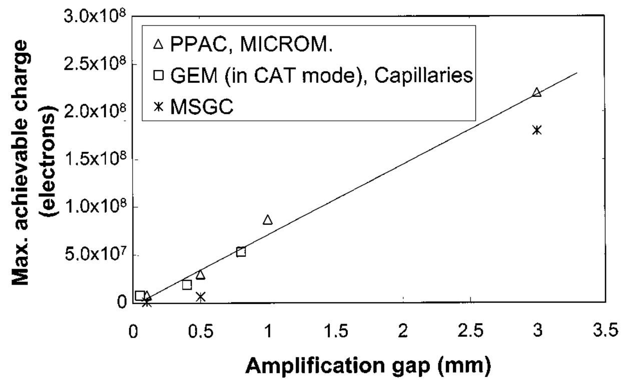

Fig. 3. Dependence of the maximum achievable charge on the amplification gap at $n_0 \sim 10^3$electrons. The measurements with PPAC were done in Ar+10% ethane, with MSGC in Xe+2% isobutilene, with MICROMEGAS in Ar+4% DME, and with GEM and capillaries in Ar+20% CO_2. The solid line is a linear fit to the PPAC data.

The capillary plates had a thickness of 0.25–0.4 mm and a capillary diameter of 50 or 100 μm. The plates were treated with hydrogen to decrease their resistivity [10].

PPACs were tested with three main designs of the cathode electrode: 1) metallic mesh; 2) flat well-polished metallic sheet; and 3) glass and ceramic plates with an evaporated metallic layer.

In the case of RPCs also two main cathode designs were tested: 1) metallic mesh or 2) well-polished sheet made of semiconductive materials. For these, we used Pestov glass, ceramics, and n- or p-type silicon with different doping levels. The anode plates of the RPCs and of some custom-made MICROMEGAS were also manufactured from Pestov glass or Si and were lithographically covered with aluminum or chromium strips at 30–50 μm pitch. Similar plates were also used for the position-sensitive readout of GEMs and capillary tubes, with the strips being connected to charge-sensitive amplifiers. The gap between the upper drift electrode and the detector varied from 3 to 11 mm, and the transfer gap between detectors in multistep configuration varied from 1 to 3 mm. Further details can found in [11].

III. Results at 1 atm

A. Very Low Rate

It was established earlier [3] that at very low counting rates, to below 1 Hz/mm^2, the maximum achievable charge [(MAC)—the amount of total charge in the avalanche at which breakdown appears] of micropattern detectors is determined by the Raether limit

$$An_0 < 10^8 \text{ electrons} \tag{1}$$

where A is the gas gain and n_0 is the number of primary electrons. Measurements presented in this paper confirm that in general, this statement is correct and reveal some important details.

It should be understood, however, that in practical situations, to avoid an excessive number of potentially damaging sparks, one has to work at gas gains one or two orders of magnitude smaller than the gains that correspond to the MACs presented here.

As an example, Fig. 2 shows the typical dependence of the MAC on n_0. One can see that the Raether limit is reached only for PPACs and $n_0 > N_{\rm crit}$, with $N_{\rm crit} \sim 10^3$ electrons. In this situation, for quencher concentrations larger than a few percent, the MAC only slightly depends on gas mixture.

For $n_0 < N_{\rm crit}$, the MAC can be orders of magnitude smaller than the Raether limit. At these values of n_0 the MAC may strongly depend on gas mixture. Moreover, it is typical of micropattern detectors that at small n_0 the MAC achieves a maximum in gas mixtures having a large value of $d(\ln A)/dV$, where V is the applied voltage (see [8], [9], and [12] for more details). These are usually helium- and neon-based mixtures with a small concentration of a quencher gas.

Qualitatively the same dependence of the MAC versus n_0 was found for all tested detectors (see results and figures in [11]).

Fig. 3 shows the typical dependence of the MAC on the gap thickness for several detector types, with $n_0 \sim N_{\rm crit}$. The MAC increases almost linearly with the gap width, leading to larger values for the thick gap gaseous detectors (wire or PPAC type) when compared to the micropattern detectors. Actually, the Raether limit (1) is only met by thick-gap PPACs. Earlier results concerning this type of detector can be also found in [13].

B. Rate Effect

It was discovered earlier that the MAC of micropattern detectors drops with counting rate (see, for example, [3] and references therein).

Two hypotheses have been suggested to explain this effect. One is based on the possible contribution of "hot" regions (regions with higher local electric fields near the cathode) to the overall multiplication process [14]. The other one is based on the "cathode excitation effect" [4], [15].

To address this problem, we performed MAC versus counting rate measurements in several PPAC designs that differ only in the nature of the cathode electrode. In one case, the cathode was manufactured from wire mesh, and in the other cases from a well-polished metallic plate and glass and ceramic plates with vacuum evaporated metallic layers, with the results shown in Fig. 4. Careful microscope exams are performed before and after the test to verify that the second detector does not have any spots on the cathode surface capable to provoke sparks. However, as

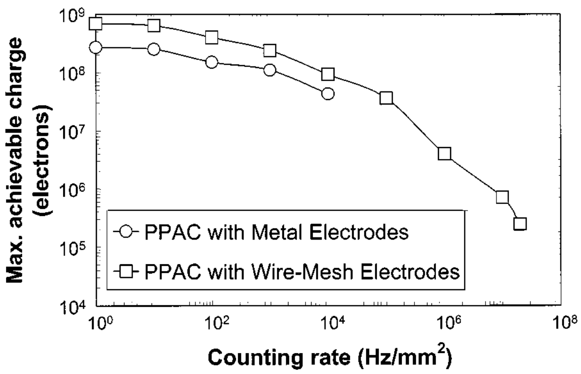

Fig. 4. Maximum achievable charge as function of counting rate for two configurations of PPAC. In both cases, the gap was 2 mm and the gas mixture Ar+20% ethane.

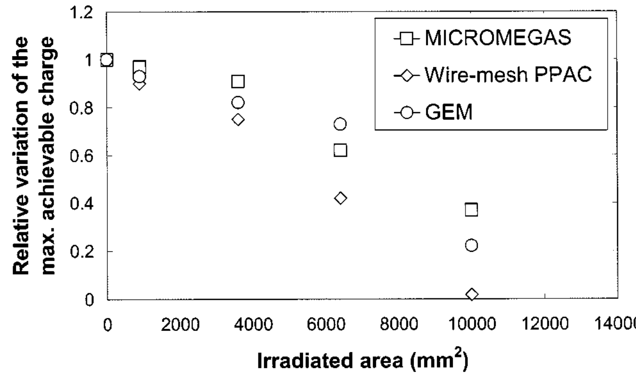

Fig. 6. Relative variation of the maximum achievable charge versus the irradiated detector area ("area effect"), measured at a flux density of 10^5 Hz/mm^2 of 20-keV X-rays in a gas mixture of Ar+20% CO_2.

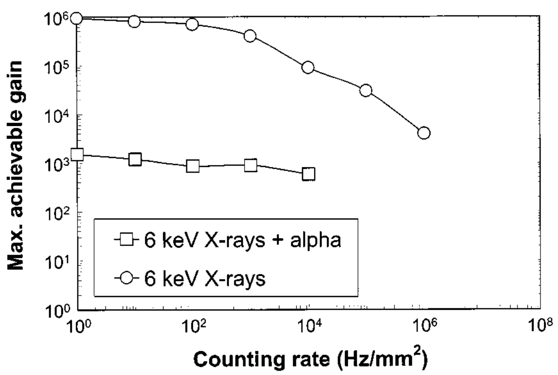

Fig. 5. Maximum achievable gain versus rate for 6-keV photons alone and in presence of a collimated alpha source ($\sim 10^3$ Hz). The measurements were made in a PPAC with 3-mm gap and 2-cm drift in a gas mixture of Ar+12% ethane.

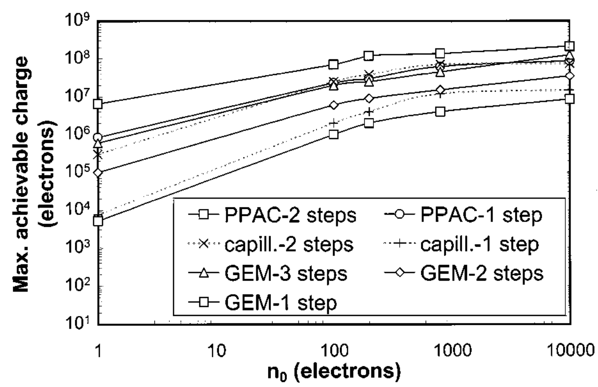

Fig. 7. Maximum achievable charge versus n_0 for several detectors, single and multistep: single GEM (in CAT mode), double GEM, triple GEM, capillary plate 0.4 mm thick, double capillary plate, PPAC 1 mm gap, double PPAC. The measurements with PPAC were done in Ar+10% ethane and with GEM and capillaries in Ar+20% CO_2.

one can see from Fig. 4, the MAC drops with rate identically for both detectors.

Note that the results presented above were obtained at small n_0 ($\sim$220 electrons); at larger n_0 (larger than 10^4 electrons), breakdown is certainly dominated by another, space charge, mechanism (see Fig. 5).

Therefore in a real experiment, the maximum achievable gain (MAG) will mostly be restricted not by the high-rate events, with small n_0, but by heavily ionizing particles.

C. Area Effect

Another important effect is that the MAG drops not only with rate but also with the irradiated area. This effect was first discovered in PPAC [3] and confirmed for GEMs [16], but qualitatively similar results were obtained later for all tested detectors [11] (see Fig. 6). This effect should be taken into account when planning a large-scale experiment.

D. Multistep Configurations

As illustrated in the previous section, the MAC of micropattern detectors is rather limited, especially at small n_0. A possibility to exceed this apparent limit is to use one or more steps of multiplication. To study the reasons for this effect, we tested most of the micropattern detectors mentioned in Section III-A in two configurations: multistep with transfer gaps in between and without them (amplification structures immediately attached to each other).

1) Multistep Configurations With Transfer Gaps: Fig. 7 shows how the MAC depends on n_0 for a number of cascaded detectors. One can see that at large n_0, in first approximation, the MAC increases linearly with the number of steps and also with the thickness of the transfer gap [11]. At small n_0, the MAC may significantly increase with the number of steps, up to several orders of magnitude.

At large n_0, the MAC depends only slightly on the gas mixture, whereas at small n_0 this dependence could be quite strong.

From the results presented in Figs. 2, 3, and 7, one can derive the interesting conclusion that in the first approximation, a few steps of "thin" detectors are more or less equivalent to one "thick" detector.

During these studie,s we also found that the ultraviolet photons emitted by the avalanches can play an important role in the operation of multistep detectors, but a detailed description of this phenomenon is out of the scope in this paper and is given in [11]. We will only briefly mention that at high gas gains, avalanche photoemission may cause the following effects: 1) longitudinal spread of the charge cloud entering the transfer region from the detector and 2) discharge propagation from one detector to another one.

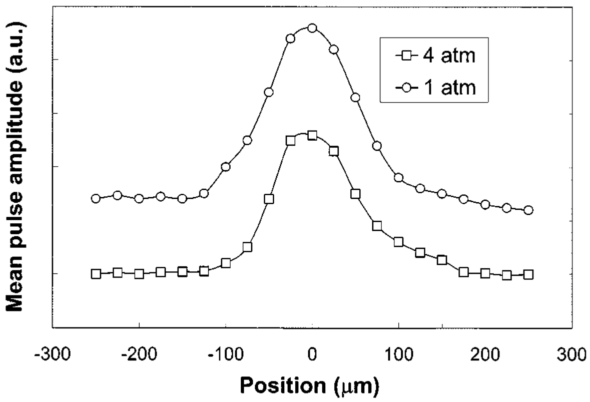

Fig. 8. The mean amplitude of the signals from a 50-μm anode strip versus position of the 50-μm collimator at two different pressures in Kr+20% CO_2. The resolution improvement is significant but small in absolute terms because it is convoluted with the strip and collimator widths.

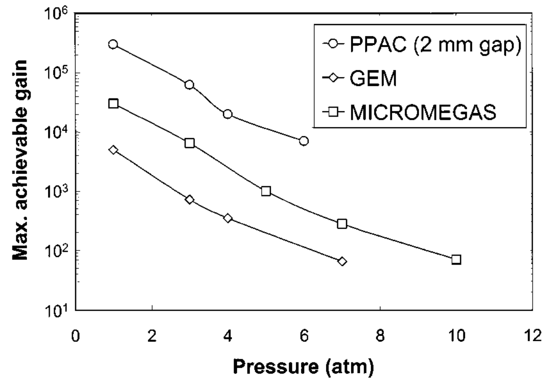

Fig. 9. Typical dependence of the maximum achievable gain as a function of pressure for several detector types. All measurements were done in Xe+40%Kr+CO_2.

The first effect (together with the enhanced diffusion effect [19]) causes a reduction of the ion density in the charge cloud moving into the transfer region, allowing a higher value of the MAC.

The second effect was that under some conditions, positive ions may "excite" the cathode and cause delayed breakdown [17]. An understanding of the role of the photons and ions provides concrete practical ways for counter design and gas optimization. For instance, the total gain increased and discharge propagation was suppressed when larger transfer regions were used [17].

2) Multistep Configurations Without Transfer Gaps: Multistep configurations without transfer regions gave a smaller overall gain and an easier discharge propagation. However, this type of detector design may be attractive for some applications such as tracking.

During these studies, we found that when the parallel-plate-type preamplification structure was directly attached to any of the other detectors, the position resolution improved remarkably. For instance, a position resolution of 50 μm could be easily obtained directly from the measured analog signals of the anode strips (without applying any treatment method like the center of gravity [8], [9]). It is interesting to note, however, that a comparable position resolution could also be achieved with a large-gap RPC (see Fig. 8 and explanation in [8]).

IV. High Pressure

Detectors operating at high pressure are very attractive for some applications like medical or astrophysical measurements, being also interesting to study micropattern detectors at elevated pressures.

Fig. 9 shows the typical dependence of the MAG on gas pressure. Clearly for all detectors tested, the MAG drops strongly with pressure, while the position resolution improves with pressure (Fig. 8).

Earlier results of this type can be found in [18].

V. Discussion

A. Very Low Rate

The Raether limit is determined by the charge density in the avalanche and by its ratio with respect to the surface charge density on the detector electrodes. It is not astonishing, therefore, that at large n_0, this limit depends on the detector geometry, gap width, number of steps, and gas pressure.

At small n_0, the situation is different. In this case, one has to apply the maximum possible voltage to the detector electrodes. Thus the breakdown at small n_0 appears due to the combination of several effects: statistical fluctuations in the avalanche final charge An_0, imperfections of the detector construction (breakdown along the dielectric surfaces [12] or due to sharp edges, tips, etc.), and cosmic and ambient radioactivity. Associated to these effects, there are also electron jets from the cathode surface [4]. As a result, the MAC is smaller than what may be expected from the Raether limit alone.

B. Rate Effect

As we have already mentioned, there are two hypotheses explaining the rate effect at small n_0.

The measurements presented in Fig. 4 seem to exclude the hypothesis based on "hot" regions and therefore indirectly support alternative explanations, for instance, the explanation given in [4]. According to this "cathode excitation" hypothesis, for optimized detector rate characteristics one should use gases with no polymerization and no adsorbed layers [4].

C. Multistep Configurations

At large n_0, breakdown due to the space charge mechanism dominates and a possibility to improve the total gain is to use a large gap detector or a multistep configuration. These small gain improvements are due to the enhanced charged cloud diffusion [19] and to the avalanche spread due to photons.

At small n_0, however, the increase in MAC can be considerable because each detector step operates at a voltage lower than the possible maximum, reducing many of the deleterious effects mentioned above.

These effects are also particularly sensitive to gas composition, which has a noticeable effect only at small n_0.

D. Comparison With the Large-Gap Detectors

It follows from our data that a multistep micropattern detector configuration is equivalent, in first approximation, to a single thick-gap detector. It is therefore interesting to compare micropattern detectors with the traditional large-gap detectors: wire and parallel-plate types.

Wire detectors (single or multi) usually do not suffer from destructive sparks, transiting at high gains from an avalanche mode of operation to a Geiger mode or a quenched streamer mode. However, these detectors have reduced time and position resolutions, while RPCs, being also protected against damaging discharges, enjoy an excellent time (50 ps σ [20]) and position resolution (30 to 50 μm full-width half-maximum [9], [21]), with high counting rates also being possible (10^5 Hz/mm^2 [22]).

E. How Could the Micropattern Detectors Be Improved?

Summarizing our results, it follows from Figs. 2–7 that at $n_0 > N_{\rm crit}$, no important improvements in the maximum achievable charge are possible, as the maximum achievable charge is set by the space charge effect. However, some modest improvements are possible by increasing the gap width or by using a few steps of multiplication. By using semiconductive electrodes, one can restrict the destructive power of any occasional sparks.

At small n_0, the use of the multistep configuration or wide-gap detectors is crucial in order to reach high gains. Some additional improvements could be gained through the gas (large $d(\ln A)/dV$) and detector geometry optimization (geometries insuring fast drop of the electric field with the distance from the anode [12]).

In tracking applications, it is important to minimize the size of the induced charge region on the detector's electrodes in order to improve the position resolution. Unfortunately, in the case of the wide-gap detectors or multistep configuration, the size of the induced signal region increases, but in some applications one can improve this parameter by using a preamplification gap.

In general, a compromise exists between the composition of the gas mixture, the maximum achievable gain (especially at small n_0), and the size of the charge-induced region. A detailed description of several optimized configurations of micropattern detectors that we successfully used for high-rate applications can be found in [8], [9], and [11]. One of them, MICROMEGAS with preamplification region, is now considered as a tracker detector for several large-scale experiments at CERN [23].

VI. CONCLUSIONS

We have described several effects have an impact, sometimes strong, on the maximum achievable gain of gaseous detectors: amount of primary charge, total and local counting rate, presence of heavily ionizing radiation, number of amplification steps, and gas pressure.

The complex and often counterintuitive interplay of all these factors excludes the possibility of an optimum solution, applicable to all situations, with a few guidelines sketched in the discussion.

In some applications, it is our opinion that RPCs are excellent. Being protected from damaging discharges by the resistive electrodes, they feature high gain, high rate capability, good position resolution, and excellent timing.

ACKNOWLEDGMENT

The authors would like to thank F. Sauli and L. Ropelewski for discussions and comments on the manuscript.

REFERENCES

[1] F. Sauli, "Gas detectors: Recent developments and future perspectives," *Nucl. Instrum. Meth.*, vol. A419, pp. 189–201, 1998.

[2] A. Sharma, "Gaseous micropattern detectors in astrophysics, radiology and plasma physics," presented at the IEEE Nuclear Science Symp. Medical Imaging Conf., Lyon, France, 2000.

[3] Y. Ivaniouchenkov, P. Fonte, V. Peskov, and B. D. Ramsey, "Breakdown limit studies in high-rate gaseous detectors," *Nucl. Instrum. Meth.*, vol. A422, pp. 300–304, 1999.

[4] P. Fonte, V. Peskov, and B. Ramsey, "The fundamental limitations of high-rate gaseous detectors," *IEEE Trans. Nucl. Sci.*, vol. 46, pp. 312–315, 1999.

[5] A. Bressan, M. Hoch, P. Pagano, L. Ropelewski, M. Gruwe, and A. Sharma *et al.*, "High rate behavior and discharge limits in micropattern detectors," *Nucl. Instrum. Meth.*, vol. A424, pp. 321–329, 1999.

[6] B. Schmidt, private communication , University of Heidelberg.

[7] R. Bellazzini, private communication , INFN, Pisa.

[8] V. Peskov and P. Fonte, "Gain, rate and position resolution limits of micropattern detectors," in *Proc. Int. Workshop Micropattern Detectors*, Orsay, France, 1999, pp. 55–58.

[9] P. Fonte and V. Peskov, "Micro-gap parallel-plate chambers with porous secondary electron emitters," *Nucl. Instrum. Meth.*, vol. A454, pp. 260–266, 2000.

[10] V. Peskov, E. Silin, T. Sokolova, and I. Rodionov, "Glass capillary plate—A new high granularity gaseous detector of particles and photons," *IEEE Trans. Nucl. Sci.*, vol. 47, pp. 1825–1828, 2000.

[11] V. Peskov, P. Fonte, M. Danielsson, C. Iakobaeus, J. Ostling, and M. Wallmark, "Fundamentals of micropattern detectors," LIP, Coimbra, Portugal, preprint LIP/01-5.

[12] P. Fonte, V. Peskov, and B. D. Ramsey. (1997, Fall) Streamers in MSGC's and other gaseous detectors. *ICFA Instrum. Bull.* [Online]. Available: http://www.slac.stanford.edu/pubs/icfa. vol. 15

[13] Y. Raizer, *Gas discharge physics*. Berlin, Germany: Springer-Verlag, 1997.

[14] F. Sauli and L. Ropelewski, private communication, 1998, CERN, Montreal.

[15] P. Fonte, V. Peskov, and B. D. Ramsey. (1998, Summer) Which gaseous detector is the best at high rates. *ICFA Instrum. Bull.* [Online]. Available: http://www.slac.stanford.edu/pubs/icfa. vol. 16.

[16] J. Ostling, A. Brahme, M. Danielsson, C. Iacobaeus, and V. Peskov, "Amplification and conditioning properties of GEM and CAT detector for beam monitoring," in *Proc. Int. Workshop Micropattern Detectors*, Orsay, France, 1999, pp. 143–148.

[17] M. Walmarkt, "Operating range of a GEM for portal imaging," diploma thesis, KTH, Stockholm, Sweden, 2000.

[18] F. A. F. Fraga, M. M. F. R. Fraga, R. F. Marques, L. M. S. Margato, J. R. Gonçalo, A. J. P. L. Policarpo, C. W. E. Eijk, R. W. Holander, and J. Van der Marel, "Perfomance of microstrip and microgap gas detectors at high pressure," *Nucl. Instrum. Meth.*, vol. A392, pp. 135–138, 1997.

[19] P. Fonte, V. Peskov, and B. D. Ramsey, "A study of breakdown limits in microstrip gas counters with preamplification structures," *Nucl. Instrum. Meth.*, vol. A416, pp. 23–31, 1998.

[20] P. Fonte, R. Ferriera Marques, J. Pinhão, N. Carolino, and A. Policarpo, "High-resolution RPC's for large TOF systems," *Nucl. Instrum. Meth.*, vol. A449, pp. 295–301, 2000.

[21] E. C. Zeballos, I. Crotty, P. Fonte, D. Hatzifotiadou, J. L. Valverde, and V. Peskov *et al.*, "New developments of RPC: Secondary electron emission and microstrip readout," *Sci. Acta*, vol. XI-1, pp. 45–49, 1996.

[22] P. Fonte, N. Carolino, L. Costa, R. Ferreira-Marques, S. Mendiratta, and V. Peskov *et al.*, "A spark-protected high rate detector," *Nucl. Instrum. Meth.*, vol. A431, pp. 154–159, 1999.

[23] Y. Giomataris, private communication , DAPNIA, Saclay.

[24] A. Sharma. Gaseous micropattern detectors in astrophysics, radiology and plasma physics. [Online]. Available: http://weblib.cern.ch/abstract?CERN-OPEN-2000—313.